Kinetic Model for the Thermal Rearrangement of *cis*- and *trans*-Pinane†

Achim Stolle,‡ Werner Bonrath,‡,§ Bernd Ondruschka,*,‡ Daniel Kinzel,|| and Leticia González||

Institute for Technical Chemistry and Environmental Chemistry, Friedrich-Schiller University Jena, Lessingstrasse 12, D-07743 Jena, Germany, R&D Chemical Process Technology, DSM Nutritional Products, P.O. Box 2676, CH-4002 Basel, Switzerland, and Institute for Physical Chemistry, Friedrich-Schiller University Jena, Helmholtzweg 4, D-07743 Jena, Germany

Received: January 31, 2008; Revised Manuscript Received: April 4, 2008

On the basis of pyrolysis experiments with *cis*-pinane (**1a**), *trans*-pinane (**1b**), *β*-citronellene (**2**), and isocitronellene (**3**), rate constants and activation parameters for the thermal rearrangement of the title compounds were calculated. Combining these with experimental parameters (residence time) allows for the kinetic modeling of the thermal rearrangement of **1a**, **1b**, **2**, and **3**. The chosen model of competitive first-order reactions describes the thermal behavior of the title compounds in a very good manner over a wide temperature range.

Introduction

The gas-phase isomerization of monoterpenes like α-pinene or pinanol plays a major role in the industrial synthesis of building blocks for the production of vitamins, flavors and fragrances as well as for the synthesis of chiral auxiliaries.[1–5] Thermally induced rearrangements of molecules in the pinane series (pinane, α-pinene, pinanol) lead to the formation of acyclic products (*β*-citronellene, alloocimene, linalool) and, depending on the substitution pattern, to monocyclic *p*-menthane-type compounds (limonene).[4,6,7] Literature reports kinetic data for the isomerization of α-pinene, *β*-pinene and 2-pinanol, but there is little work published describing the rearrangement of pinane (**1**), the saturated eponym for this type of natural products.[4–6]

β-Citronellene (**2**) and isocitronellene (**3**) are the main products yielding from pinane thermal isomerization.[7–9] Monocyclic *p*-menthane-type compounds are reported to be present in the reaction mixtures only in low amounts.[8,9] Acyclic products **2** and **3** and monocyclic reaction products seem to originate from stepwise fragmentation of the cyclobutane ring via biradical intermediates. The thermal treatment of **2** and **3** leads to formation of substituted cyclopentenes via ene-reactions.[8–13]

Herein, kinetic parameters for the thermal isomerization of *cis*-pinane (**1a**) and *trans*-pinane (**1b**) are presented. Besides the formation of the primary products *β*-citronellene (**2**), isocitronellene (**3**) and *p*-menthene isomers, also consecutive reactions of **2** and **3** leading to substituted cyclopentenes **4** and **5**, respectively, were taken into account. On the basis of the calculated Arrhenius-parameters for the reactions contributing to the isomerization reactions of both pinane isomers, a kinetic model is presented, describing the temperature dependent mole fractions within the rearrangement process considering reaction parameters like flow rate or reactor volume. In addition, it is shown that the model is suitable for the prediction of the temperature dependent behavior of mixtures of the two pinane isomers with different molar ratio.

Experimental Section

Materials. (+)-*cis*-Pinane (**1a**, ca. 99%), (−)-*trans*-pinane (**1b**, ca. 99%), (−)-*β*-citronellene (**2**, ca. 95%), and (+)-isocitronellene (**3**, ca. 99%) were purchased from Fluka and were used without further purification. Purity was determined by capillary gas chromatography.

Kinetic Experiments. A detailed description of the apparatus used herein can be found in literature.[6,14] The kinetic experiments were carried out in temperature ranges from 450 to 512, 500 to 550, 462 to 550, and 487 to 537 °C for **1a**, **1b**, **2**, and **3**, respectively. Dilution gas pyrolysis was carried out in an electrically heated quartz tube of 500 mm length and with a pyrolysis zone of approximately 200 mm, using the apparatus described previously.[14] In all experiments, oxygen-free nitrogen with a purity of 99.999% was used as the carrier gas. Variation of the carrier gas velocity in a range from 0.25 up to 1.2 L/min N_2 allows for the modulation of the average residence time. The substrates (15 μL) were introduced onto a quartz ladle at the top part of the pyrolysis apparatus using a glass syringe (50 μL) and carried along with the nitrogen stream into the reactor. Vaporization of the starting material was supported by heating the ladle to 200 °C with a hot blast. Pyrolysis products were collected in a cold trap (liquid nitrogen) and were dissolved in 1.5 mL of ethyl acetate. Analyses of those with GC-FID were carried out with a 6890 Series GC from Agilent Technologies. Comparison of both residence times and mass spectra with those of reference compounds allowed for identification of the products.[9] GC-FID: HP 5; 30 m × 0.32 mm × 0.25 μm; H_2, 5 psi; program 35 °C (hold 1 min), 4 K/min up to 80 °C, 4.5 K/min up to 90 °C, 35 K/min up to 280 °C (hold 3 min); injector temperature, 250 °C; detector temperature, 280 °C. Calibration of the FID-detector for **1a**, **1b**, **2** and **3** with hexadecane as an internal standard showed no significant differences in detector response for the different reactants.

Thermodynamic Data. The geometries of **1a**, **1b**, **2**, and **3** were optimized using the Complete Active Space Self Consistent Method[15] CASSCF/6-31G** using four electrons in the four $\pi\pi^*$ orbitals of **2** and **3** and the corresponding $\sigma\sigma^*$ orbitals of **1a** and **1b**. The frequency calculation and the thermodynamic analysis leading to absolute enthalpies *H* and entropies listed in Table 1 have been done at the same level of theory. The optimized geometries can be found in the Supporting Informa-

† For a report on the first part of this study, see ref 9.

* Corresponding author. Phone: +49 3641 948400. Fax: +49 3641 948402. E-mail: bernd.ondruschka@uni-jena.de.

‡ Institute for Technical Chemistry and Environmental Chemistry, Friedrich-Schiller University Jena.

§ DSM Nutritional Products.

|| Institute for Physical Chemistry, Friedrich-Schiller University Jena.

10.1021/jp800916b CCC: $40.75
Published on Web 06/06/2008

TABLE 1: CASSCF(4,4)/6-31G Thermodynamic Data for the Pyrolyzed Compounds**

entry	compound	T (K)	G^T (au)	H^T (au)	S^T (J mol^{-1} K^{-1})
1	*cis*-pinane (**1a**)	750	−389.0362	−388.8534	152.9
2	*trans*-pinane (**1b**)	800	−389.0566	−388.8538	159.1
3	β-citronellene (**2**)	750	−389.0805	−388.8700	176.1
4		800	−389.0948	−388.8622	182.4
5	isocitronellene (**3**)	750	−389.0724	−388.8639	174.5
6		800	−389.0866	−388.8561	180.8

TABLE 2: Thermodynamic Data for the Formation of β-Citronellene (2) and Isocitronellene (3) from *cis*-Pinane (1a) and *trans*-Pinane (1b)

reaction	T (K)	$\Delta_R H^T$ (kJ mol^{-1})	$\Delta_R S^T$ (J mol^{-1} K^{-1})	$\Delta_R G^T$ (kJ mol^{-1})
1a → **2**	750	−43.6	97.1	−116.4
1a → **3**	750	−27.5	90.2	−95.2
1b → **2**	800	22.1	97.9	−100.5
1b → **3**	800	−6.0	91.1	−78.8

SCHEME 1

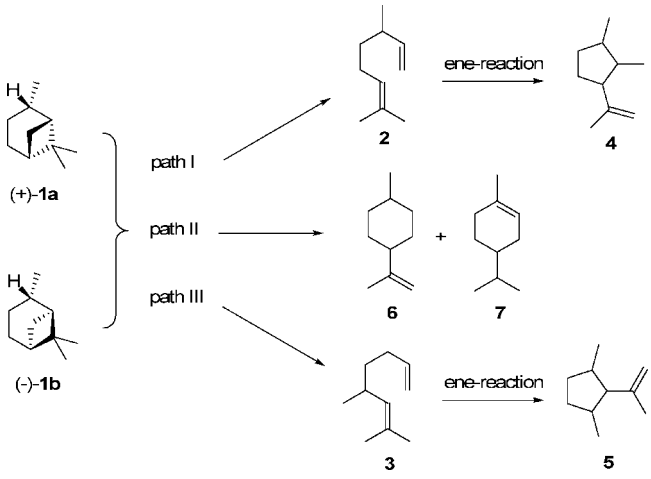

tion. The temperatures of 750 and 800 K were chosen with respect to the fact that those are the mean temperatures used for the calculation of the rate constants in the reaction networks based on **1a** and **1b**, respectively. The formation of monocyclic reaction products **6** and **7** are not considered because they were formed in very low amounts only. On the basis of eqs 1–3, the reaction enthalpies $\Delta_R H$, reaction entropies $\Delta_R S$, and Gibbs free energies $\Delta_R G$, respectively, have been calculated for the formation of **2** and **3** from both **1a** and **1b** (Table 2).

$$\Delta_R H^T = H^T_{\text{product}} - H^T_{\text{educt}} \quad (1)$$

$$\Delta_R S^T = S^T_{\text{product}} - S^T_{\text{educt}} \quad (2)$$

$$\Delta_R G^T = \Delta_R H^T - T \cdot \Delta_R S^T \quad (3)$$

Results and Discussion

Thermal Isomerization Reactions. Scheme 1 illustrates the reaction network for the thermal isomerization of pinane (**1**). The main reaction products are β-citronellene (**2**) and isocitronellene (**3**), which are formed with an overall selectivity of 95% (Scheme 1). Stepwise fragmentation of the cyclobutane ring in **1** seems to be the explanation for the formation of both acyclic isomers, because concerted [2+2]-cycloadditions as well as [2+2]-cycloreversions are thermally forbidden with respect to the Woodward−Hoffmann rules. Apparently these products

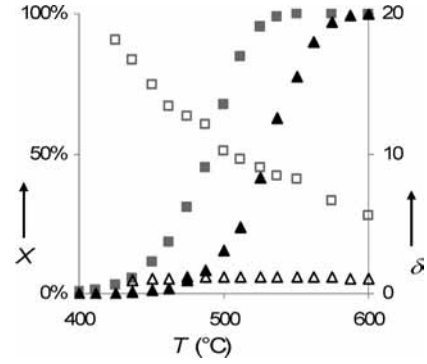

Figure 1. Conversion (X; filled symbols) and **2/3** ratio (δ; empty symbols) vs T for the thermal isomerization of *cis*- (**1a**; squares) and *trans*-pinane (**1b**; triangles).

yield from reaction pathways passing through biradical intermediates (path I and III; Scheme 1) as described in the literature for the formation of ocimene or myrcene from α- or β-pinene, respectively.[4,6,7,9] Besides **2** and **3**, also monocyclic *p*-menthene type compounds (**6**, **7**) were identified in the reaction mixtures.[9]

Consecutive reactions of **2** and **3** are the reason for a decrease in their yield at elevated temperatures. Via ene-reactions, substituted cyclopentanes **4** and **5** are formed from **2** and **3**, respectively. Within the cyclization process two new chiral centers are built in **4** and **5**, whereas it was shown that the configuration of the chiral carbon atom in **2** and **3** remains unchanged.[8–10] Therefore, these cyclization products are built in four different diastereomeric forms. Because of the fact that only the isomerization of **1** to the acyclic isomers and their loss due to consecutive reactions is interesting for the kinetic model, the formation of those diastereomeric compound is neglected in the presented kinetic model.

It is well-known but rarely discussed in literature that the two diastereomeric forms of **1** differ in reactivity and selectivity of the primarily formed isomerization products.[8,9] The temperatures corresponding to complete conversion of the *cis*-isomer (**1a**) and *trans*-pinane (**1b**) are 550 and 600 °C, respectively, underlining the higher reactivity of the *cis*-isomer (Scheme 1, Figure 1). Equation 4 introduces the parameter δ as the ratio of path I to path III. Besides the higher reactivity of **1a**, Figure 1 also points out the different behavior concerning selectivity for the formation of the two acyclic isomers **2** and **3**. Whereas thermal treatment of **1a** leads to δ of 18.2 at 425 °C decreasing to 5.5 as the temperature increases up to 600 °C, the ratio remains at a constant level of 1.0−1.2 over the whole temperature range within the thermally induced rearrangement of **1b**. Hence, **1a** leads to the formation of **2** as the overall main product and by changing the relative configuration of one carbon-atom (**1b**), **2** and **3** are formed in equal amounts.

$$\delta = \frac{\text{path I}}{\text{path III}} = \frac{[\mathbf{2}] + [\mathbf{4}]}{[\mathbf{3}] + [\mathbf{5}]} \quad (4)$$

Kinetic Studies. Variation of the carrier gas velocity in the pyrolysis apparatus allowed us to set up various average residence times τ. Calculation of the residence times are described by eq 5, whereas V_R is the reactor volume, V^*_E the substrate flow rate, $V^*_{N_2}$ the carrier gas flow rate, T_R and T_{rt} are the reactor and ambient temperature, both in K.

$$\tau = \frac{\dot{V}_R}{(\dot{V}_E + \dot{V}_{N2})\dfrac{T_R}{T_{rt}}} \quad (5)$$

For calculation of the residence times and rate constants, it had to be ensured that no gaseous products were formed and

that the liquid pyrolysis products were completely condensed. The reaction products did not undergo further degradation to lower molecular weight products and were able to be trapped completely in the temperature range in which the conversion of the starting material (**1a**, **1b**, **2**, **3**) increases linearly with rising the temperature (Figure 1). A high carrier gas to substrate ratio (e.g., 3000 at 500 °C) suppresses bimolecular reactions leading to dimers, oligomers and coke. Thermally induced cyclobutane fragmentations and ene-reactions are unimolecular reactions; therefore, first-order kinetics were chosen to describe the rearrangements of both bicyclic and acyclic products. Kinetic experiments with **1a** and **1b** were carried out to describe the rearrangements of the bicyclic starting materials to the primarily formed products (**2**, **3**, **6**, **7**). Due to their low concentration the *p*-menthene type pyrolysis products **6** and **7** are summarized as monocyclic products (**mc** = **6** + **7**). The corresponding parts resulting from consecutive reactions (**4**, **5**) were added to the respective primarily formed products (**2**, **3**). Studying the thermal rearrangement of **2** and **3** allows for the estimation of rate constants for the isomerization of the acyclic substrates yielding **4** and **5**, respectively. The parallel first-order reaction model was chosen to describe the thermal behavior of the compounds investigated. General rate equations used for the description of disappearance of starting materials (k_d) are given in eq 6, wherein [A] is the substrate concentration (**1a**, **1b**, **2**, **3**). Due to the fact that for parallel first-order reactions the sum of the rate constants for each reaction channel leading to product P (k_P) equals the overall rate constant for the disappearance of the starting material (k_d; eq 7) allows in combination with the mass balance (eq 8) for setting up the general equation describing the formation of *P* (eq 9).

$$\frac{d[A]}{d\tau} = -k_d[A] \Rightarrow [A] = [A]_0 e^{-k_d\tau} \quad (6)$$

$$k_d = \sum k_P \quad (7)$$

$$[A]_0 + \sum [P]_0 = [A] + \sum [P] = 1 \quad (8)$$

$$\frac{d[P]}{d\tau} = k_P[A] \Rightarrow [P] = [P]_0 + \frac{k_P[A]_0}{k_d}(1 - e^{-k_d\tau}) \quad (9)$$

Plotting ln[A] against τ and linear regression leads to the rates constants k_d for the disappearance of starting materials **1a**, **1b**, **2**, **3**, which are given in the Supporting Information. On the basis of k_d for **1a** and **1b** and consideration of eqs 7–9, the rate constants for the formation of the products **2**, **3**, and **6** + **7** (**mc**) yielded from isomerization of **1** (Scheme 1) were calculated using eqs 10–12, respectively.

$$k_2 = k_d \cdot \frac{[2] + [4]}{[2] + [3] + [4] + [5] + [6] + [7]} \quad (10)$$

$$k_3 = (k_d - k_2) \cdot \frac{[3] + [5]}{[3] + [5] + [6] + [7]} \quad (11)$$

$$k_{mc} = k_d - k_2 - k_3 \quad (12)$$

Determination of various rate constants by performing kinetic pyrolysis experiments at various temperatures, allows for the calculation of both Arrhenius (E_a, $\log_{10} A$) and Eyring parameters ($\Delta H^{\#}$, $\Delta S^{\#}$), eqs 13 and 14. Simplification of the Arrhenius equation was possible because the reaction volume remains constant and no further gaseous degradation products were detected ($\Delta V = 0$). Calculation of the Arrhenius and Eyring parameters was performed by simply plotting ln k_T or ln(k_T^{-1}), respectively, against inverse reaction temperature T^{-1} in K^{-1}.

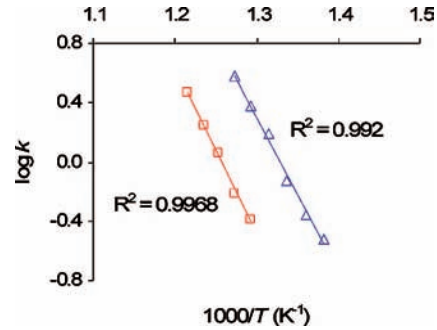

Figure 2. Arrhenius plot of 1000/*T* vs log *k* for the thermal isomerization of *cis*- (**1a**; triangles) and *trans*-pinane (**1b**; squares).

Arrhenius plots for the conversion of the bicyclic substrates **1a** and **1b** are shown in Figure 2.

$$k_T = Ae^{(-1/RT)(E_a + 0.1\Delta Vp)} \quad (13)$$

$$k_T = \frac{k_B T}{h} \cdot e^{-\Delta H^{\#} - T\Delta S^{\#}/RT} \quad (14)$$

Table 3 lists the calculated activation parameters for both the Arrhenius equation (13) and the Eyring equation (14) calculated from the linearized forms of the equations using the slope and axis intercepts of the linear regression functions for the gas-phase isomerization reactions of **1a** and **1b** (Figure 2). The lower activation energy E_a for the transformation of **1a** (201 kJ mol^{-1}) compared to **1b** (213 kJ mol^{-1}) underlines the higher reactivity of the *cis*-isomer (Figure 1). Weigand and Schneider reported ring-strain energies (E_{strain}) of **1a** and **1b** compared to norpinane (**8**) based on ab initio calculations (Scheme 2).[16] The differences of $E_{strain;\mathbf{1i}} - E_{strain;\mathbf{8}}$ ($\Delta_{\mathbf{1i\text{-}8}}$) are listed for both isomers in Table 4. Comparison of the absolute differences between $\Delta_{\mathbf{1a\text{-}8}}$ and $\Delta_{\mathbf{1b\text{-}8}}$ shows high accordance to the difference in E_a (last column in Table 4). Therefore, the higher reactivity of **1a** is due to its higher E_{strain}. The ground-state confirmation of the cyclohexane ring in case of **1a** is a semichair confirmation wherein the methyl group is semiequatorial, whereas the chair confirmation with an equatorial methyl group is the preferred ground-state geometry for **1b**.[16]

Comparison of E_a for the formation of the acyclic products **2** and **3** confirms that **2** is the main product in case of **1a** ($k_{\mathbf{2(1a)}}$), whereas the equality for the pyrolysis of **1b** supports that both reaction channels are moving together (Figure 1).[8,9] The error margins of the reported activation parameters reflect the typical experimental uncertainty with error limits of ±8.3 kJ mol^{-1} in the activation energy E_a and ±0.7 in $\log_{10}A$ being reported as typical for gas-phase thermal decomposition reactions.[17,18]

Whereas the values for $\Delta S^{\#}$ for the formation of pyrolysis products listed in Table 3 display large variations, the activation entropies for the rearrangement of **1a** and **1b** reveal no significant differences, allowing for the conclusion that the transition states (TS) in both cases are only slightly different from those in the initial state.[17,18] The same conclusions can be drawn considering the formation of **2** and **3** from **1b** ($k_{\mathbf{2(1b)}}$, $k_{\mathbf{3(1b)}}$). Because all activation parameters are quite similar to those reported for $k_{\mathbf{1b}}$, the TS leading to these products (**2**, **3**) are equal to each other and to the one resulting initially from **1b**. Similar conclusions can be drawn for the formation of **2** from *cis*-pinane (**1a**), but due to the fact that $\Delta S^{\#}$ for $k_{\mathbf{3(1a)}}$ is positive and $\log_{10}A$ is higher than 14, a loose TS seems to exist for the formation of **3** from **1a**. Loose TSs are characterized by more rotational freedom or greater freedom for torsional movement than is permissible in the ordinary molecule typically

TABLE 3: Kinetic Data[a] for the Gas-Phase Isomerization Reactions of *cis*- (1a) and *trans*-Pinane (1b)

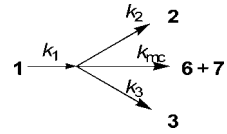

	k	E_a (kJ mol^{-1})	$\log_{10}A$ (s^{-1})	$\Delta H^{\#}$ (kJ mol^{-1})	$\Delta S^{\#}$ (J K^{-1} mol^{-1})
cis-pinane (**1a**)	k_{1a}	201.1 ± 9.1	14.0 ± 0.6	194.8 ± 9.0	6.3 ± 0.4
2	$k_{2(1a)}$	200.1 ± 9.0	13.8 ± 0.6	193.8 ± 12.0	3.7 ± 0.2
3	$k_{3(1a)}$	233.7 ± 8.3	15.1 ± 0.6	227.4 ± 8.3	28.2 ± 1.4
6 + 7 = mc[b]	$k_{mc(1a)}$	177.7 ± 10.8	11.2 ± 0.8	171.4 ± 11.0	−47.1 ± 4.5
trans-pinane (**1b**)	k_{1b}	213.0 ± 6.9	14.0 ± 0.5	206.3 ± 6.9	6.2 ± 0.3
2	$k_{2(1b)}$	213.4 ± 7.5	13.7 ± 0.5	206.7 ± 7.4	1.1 ± 0.1
3	$k_{3(1b)}$	213.9 ± 6.3	13.7 ± 0.4	207.2 ± 6.3	0.54 ± 0.02
6 + 7 = mc[b]	$k_{mc(1b)}$	201.0 ± 7.6	11.9 ± 0.5	194.4 ± 7.7	−33.8 ± 2.0

[a] Error limits are 95% certainty limits. [b] Sum of monocyclic *p*-menthene-type products (**6**,**7**).

SCHEME 2

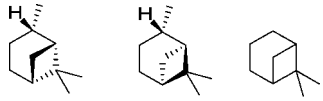

TABLE 4: Comparison of Ring-Strain Energies (E_{strain}) and Activation Energies (E_a) for *cis*- (1a) and *trans*-Pinane (1b)

	1a	**1b**	
$E_{strain;i}$ (kJ mol^{-1})[a]	166.7	158.4	
Δ_{1i-8} (kJ mol^{-1})[b]	25.4	17.1	$\Delta(\Delta_{1i-8}) = 8.3$
E_a (kJ mol^{-1})	201.1 ± 9.1	213.0 ± 6.9	$\Delta(E_a) = 11.9$

[a] Data taken from ref 16. [b] Difference between $E_{strain;i}$ of **1a** or **1b** and that of **8**. $E_{strain;8}$: 141.3 kJ mol^{-1}.

observed for the fragmentation of four-membered rings.[17–20] Those reactions often involve biradical intermediates that yield acyclic intermediates having more degrees of freedom for torsion and rotation as the cyclobutane precursor. Hence, because the $\Delta S^{\#}$ values are only slightly positive and the $\log_{10}A$ values are between 13.5 and 14 for k_{1a}, k_{1b}, k_2, and k_3 (cf. Table 3), a normal TS with similar rotational or torsional freedom as bicyclic starting material **1** is indicated. Therefore, one may conclude that the reaction probably proceeds as retro-[2+2]-cycloaddition with an 4π-antiaromatic TS. However, according to the Woodward−Hoffmann rules, those reactions are thermally forbidden and a stepwise mechanism via birdiacl intermediates is more plausible. This hypothesis is confirmed by quantum mechanical ab initio calculations.[21]

Surprisingly, the activation barriers for the formation of the *p*-menthene-type products (**6** + **7**; k_{mc}) are lower than for the formation of the other main products for both, the rearrangement of **1a** and isomerization of **1b** (Table 3). Comparison of the *A*-factors for those reaction pathways reveals that they are 3−4 orders of magnitude lower, underlining the fact that their formation apparently proceeds via different reaction intermediates,[9] whereas the acyclic main products (**2**, **3**) yield from fragmentation of the cyclobutane ring in **1**.[8,9] The reactions leading to the formation of the *p*-menthene-type products (k_{mc}) is special because negative $\Delta S^{\#}$ and $\log_{10}A$ lower than 12 suggest that a tight TS with restrictions in motion exist. Therefore, the formation of these products proceeds as a reaction with a cyclic transition state rather than a biradical. Hence, a biradical resulting from **1** (*p*-methyl-isopropyl-cyclohexene skeleton) has a larger degree of freedom than the starting material. Therefore, the formation of *p*-menthenes **6** and **7** obviously proceeds as [1,5]H-shift reaction according to the formation of acyclic enes from vinyl-substituted cyclobutanes.[22,23]

Arrhenius plots for the disappearance of both **2** (k_4) and **3** (k_5) calculated on the basis of pyrolyses with different starting materials are shown in Figure 3. On the one hand, gas-phase isomerization experiments with **2** and **3** were conducted to investigate their disappearance and on the other hand, disappearance was recalculated from pyrolyses of **1a** and **1b**. The corresponding Arrhenius and Eyring activation parameters (eqs 13,14) are listed in Table 5. Comparison of kinetic data in case of thermal isomerization of **2** (k_4) reveals huge differences in all parameters, whereas the differences in the activation parameters for pyrolysis of **3** are negligible. Nevertheless, the average values are of the same order of magnitude as those published by Huntsman and Curry for the gas-phase cyclization of **2** carried out in an apparatus similar to the one used herein (Table 5, entry 9).[13,24] Extrapolation of the linear regression function of the rate constants taken from ref 13 (black line in Figure 3a) reveals no significant differences to those rate constants found herein. Unfortunately, these cyclization reactions were rarely studied from a kinetic point of view and further data for comparison are not available. Kinetic analysis of the gas-phase isomerization of linalool (3,7-dimethylocta-1,6-dien-3-ol), a derivative of **2** with a OH-group at C(3), seems to confirm the results presented herein for the rearrangement of **2** and **3** (Table 5, entry 10). Pyrolysis experiments with linalool lead to the formation of similar reaction products as described in Scheme 1 for the pyrolyses of **2** or **3**.[25]

According to the activation parameters for k_{mc} listed in Table 3 a tight TS probably exists also for the cyclization of **2** and **3** leading to products **4** and **5**, respectively (Table 5). As already pointed out, negative values in $\Delta S^{\#}$ combined with low frequency factors are typical for six-membered-ring transition states, supporting the hypothesis that the cyclization of **2** and **3** is assumed to proceed via an ene-type reaction.[6,8,9,11–13] TS for the formation of **4** from **2** (TS2) and for cyclization of **3** yielding **5** (TS3) are shown in Scheme 3. It is also reported that the addition of radical sources or scavengers (e.g., nitrous oxide, ethylene oxide, *t*-butyl peroxide) have no effect on both reactivity and product distribution within the thermal isomerization process of **2**,[13] underlining that the reaction does not involve radical transition states.

Kinetic Model. With the help of the activation parameters presented in Tables 3 and 5 it was possible to design a kinetic model describing the temperature dependent reaction composition of the thermal isomerization reaction of both **1a** and **1b** including consecutive reactions responsible for decreasing yields of primary rearrangement products **2** and **3**. The temperature dependent rate constants for the reactions important for the

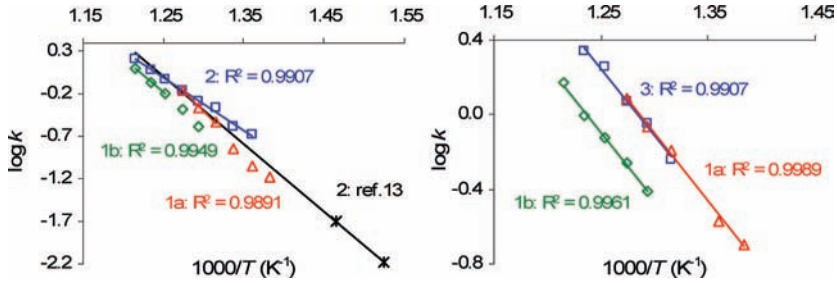

Figure 3. Arrhenius plot of 1000/T vs log k for the thermal gas-phase isomerization of β-citronellene (**2**; Figure 3a) and isocitronellene (**3**; Figure 3b). Rate constants based on pyrolysis experiments with **2** or **3** (squares), with **1a** (triangles), or with **1b** (diamonds) as substrates.

TABLE 5: Kinetic Data[a] for the Gas-Phase Isomerization Reactions of β-Citronellene (2) Leading to 4 (k_4), and of Isocitronellene (3) Yielding 5 (k_5)

entry	k	source	E_a (kJ mol^{-1})	$\log_{10}A$ (s^{-1})	$\Delta H^{\#}$ (kJ mol^{-1})	$\Delta S^{\#}$ (J K^{-1} mol^{-1})
1	k_4	pyrolysis of **2**	117.9 ± 1.6	7.7 ± 0.1	112.4 ± 4.7	−112.7± 8.0
2	k_4	pyrolysis of **1a**	136.4 ± 14.0	8.7 ± 1.0	130.3 ± 14.0	−94.8 ± 17.6
3	k_4	pyrolysis of **1b**	149.1 ± 11.1	9.6 ± 0.7	142.4 ± 11.0	−78.5 ± 9.0
4	k_4	average[b]	134	8.7	128	−95
5	k_5	pyrolysis of **3**	137.5 ± 7.3	9.2 ± 0.5	131.0 ± 7.0	−84.6 ± 7.0
6	k_5	pyrolysis of **1a**	140.2 ± 5.3	9.4 ± 0.4	133.9 ± 5.3	−80.7 ±4.9
7	k_5	pyrolysis of **1b**	139.2 ± 4.8	9.0 ± 0.3	132.6 ± 4.7	−89.3 ± 4.9
8	k_5	average[b]	139	9.2	133	−85
9	k_4	[13,24]	151	9.9	146	−70
10		linalool[c]	122	8.1	115	−107

[a] Error limits are 95% certainty limits. [b] Average of the data derived form rearrangement experiments with sole **2** or **3** and those calculated from pyrolyses of **1a** or **1b**. [c] Gas-phase pyrolysis of linalool under the same conditions; unpublished results.[25]

SCHEME 3

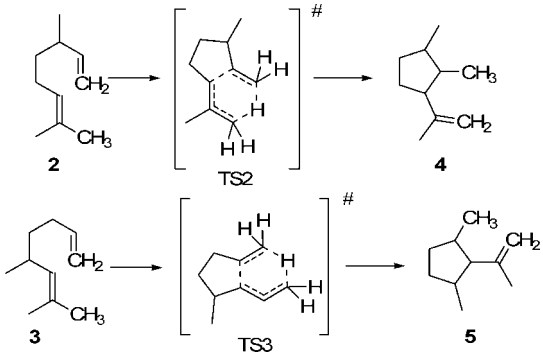

model were calculated in the range of 350 to 650 °C with an increment of 10 K (eq 13). Using the model of competitive first order reactions for the formation of the primary products **2**, **3**, and **6** + **7** (**mc**) leads to eqs 15–18 describing the mole fractions of **1**, **2**, **3**, and **mc**, respectively, for a desired reaction temperature T. Substrates (**1a**, **1b**) used within these experiments have a purity of higher than 99%. For this reason the starting concentration in the model ($[\mathbf{1}]_0$) was set 1.00 and contributing to the mass balance (eq 8) the overall molar fraction is not allowed to exceed this value. Considering experimental conditions (V_R and total volumetric flow rate) allows for the calculation of residence time τ (eq 5). $[\mathbf{4}]_T$ is calculated according to eq 19 despite the fact that the difference between **2** formed directly from **1** ($[\mathbf{2}]_{form,T}$) and the amount present in the reaction mixture $[\mathbf{2}]_T$ (eq 16) is equal to the molar fraction of **4**. Mole fraction of **5** was calculated in the same way (eq 20).

$$[\mathbf{1}]_T = [\mathbf{1}]_0 e^{-k_{1;T}\tau} \xrightarrow{[\mathbf{1}]_0 = 1} [\mathbf{1}]_T = e^{-k_{1;T}\tau} \quad (15)$$

$$[\mathbf{2}]_T = \frac{k_{2;T}}{k_{1;T}}(1 - e^{-k_{1;T}\tau})e^{-k_{4;T}\tau} \quad (16)$$

$$[\mathbf{3}]_T = \frac{k_{3;T}}{k_{1;T}}(1 - e^{-k_{1;T}\tau})e^{-k_{5;T}\tau} \quad (17)$$

$$[\mathbf{mc}]_T = \frac{k_{\mathbf{mc};T}}{k_{1;T}}(1 - e^{-k_{1;T}\tau}) \quad (18)$$

$$[\mathbf{4}]_T = [\mathbf{2}]_{form;T} - [\mathbf{2}]_T = \frac{k_{2;T}}{k_{1;T}}(1 - e^{-k_{1;T}\tau}) - \frac{k_{2;T}}{k_{1;T}}(1 - e^{-k_{1;T}\tau})e^{-k_{4;T}\tau} = \frac{k_{2;T}}{k_{1;T}}(1 - e^{-k_{1;T}\tau})(1 - e^{-k_{4;T}\tau}) \quad (19)$$

$$[\mathbf{5}]_T = [\mathbf{3}]_{form;T} - [\mathbf{3}]_T = \frac{k_{3;T}}{k_{1;T}}(1 - e^{-k_{1;T}\tau}) - \frac{k_{3;T}}{k_{1;T}}(1 - e^{-k_{1;T}\tau})e^{-k_{5;T}\tau} = \frac{k_{3;T}}{k_{1;T}}(1 - e^{-k_{1;T}\tau})(1 - e^{-k_{5;T}\tau}) \quad (20)$$

Figure 4 compares the experimental with the model data for the thermal isomerization of **1a**. Because of the high accordance between experiment and model the chosen kinetic model of competitive first-order reaction seems to be correct. The visible discrepancies are within the calculated error margins. Even though reactions leading to gaseous products were not present within the temperature range where the activation parameters were determined, it is important to point out that the model is only valid if no decomposition reactions leading to gaseous products took place. At temperatures higher than 575 °C the formation of lower molecular products was observed. Therefore, the discrepancies at elevated temperatures between experiment and model are most likely due to this fact.

With respect to the theory of microreversibility, every chemical reaction is an equilibrium reaction whereby the temperature-dependent equilibrium constant K determines the ratio of forward and back-reaction rates.[18] Under certain conditions the back-reaction (k_{back}) might be neglected whereby the reaction is controlled by the forward reaction (k_{for}) only.

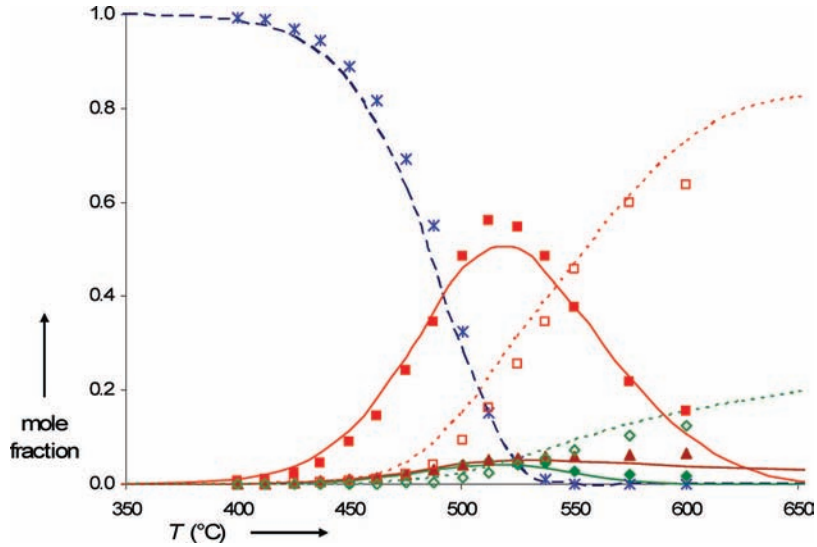

Figure 4. Mole fraction vs T for experimental data (symbols) and modeling data (lines) for the thermal isomerization of *cis*-pinane: **1a**, asterisk and dashed blue line; **2**, filled squares and red line; **3**, filled diamonds and green line; **6** + **7**, triangles and brown line; **4**, empty squares and red dotted line; **5**, empty diamonds and green dotted line.

TABLE 6: Comparison of the Rate Constants for Forward and Backward Reaction in the Case of Formation of β-Citronellene (2) and Isocitronellene (3) from *cis*-Pinane (1a) and *trans*-Pinane (1b)

reaction	T (K)	log K^T	k_{for}[a] (s^{-1})	k_{back} (10^{-9} s^{-1})
1a → **2**	750	8.11	0.776 ($k_{2(1a)}$)	6.04
1a → **3**	750	6.63	0.067 ($k_{3(1a)}$)	15.89
1b → **2**	800	6.56	0.608 ($k_{2(1b)}$)	167.81
1b → **3**	800	5.15	0.525 ($k_{3(1b)}$)	3733.91

[a] With respect to data given in Table 3.

This is possible if either the reaction is performed at a low extent of conversion or K is so much in favor of k_{for} that the influence of the back-reaction is negligible. This has to be checked by calculating K and k_{back}. The use of eq 21 in combination with the Arrhenius activation parameters listed in Table 3 and the Gibbs free energies given in Table 2 allows for estimating the equilibrium constants K and calculating of the rate constants for the backward reactions k_{back}.

$$\Delta_R G^T = -RT \ln K^T = -RT \ln \frac{k_{T;for}}{k_{T;back}} \qquad (21)$$

The corresponding values are listed in Table 6 revealing that the rate constants for the backward reactions are at least 6 orders of magnitude lower than those for the forward reactions. Thus it seems to be appropriate to neglect back-reactions when describing the formation of the acyclic main products **2** and **3** from the both bicyclic starting materials **1a** and **1b**. Taking into account the conditions at which the experiments were conducted (low τ, high T) and the fact that no bicyclic product was formed when **2** or **3** have been pyrolyzed, it is evident that the backward reactions can be ignored. Furthermore, it should be noted that the fact that the reactions pass through biradical transition states is neglected.[21]

Table 3 reports kinetic data achieved from thermal isomerization of either pure **1a** or **1b**. Therefore, Figure 4 illustrates the comparison between experiment and model for the reaction of sole **1a** without the presence of **1b**. To test the model in the case that both **1a** and **1b** are present in the starting mixture, pyrolysis experiments were conducted with substrates differing in their content of **1a** and **1b**. Parameter γ is the ratio of **1a** to **1b** and γ_0 is the initial ratio of the starting material. The ratio at reaction temperature T (γ_T) was calculated according to eq 22. The temperature dependency of γ for three different γ_0 is illustrated in Figure 5. It is shown that the model is able to predict the correct values over the whole investigated temperature range. In all cases γ drops with increasing temperature, representing the higher reactivity of **1a** compared to the *trans*-isomer **1b**.

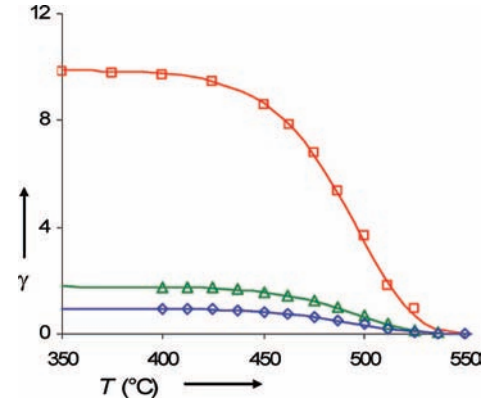

Figure 5. Ratio of *cis*- (**1a**) to *trans*-pinane (**1b**) γ vs T for experimental data (symbols) and modeling data (lines) for different initial concentrations: γ_0 = 9.87, squares and red line; γ_0 = 1.77, triangles and green line; γ_0 = 0.94, diamonds and blue line.

$$\gamma_T = \frac{[\mathbf{1a}]_T}{[\mathbf{1b}]_T} = \frac{[\mathbf{1a}]_0 e^{-k_{1a;T}\tau}}{[\mathbf{1b}]_0 e^{-k_{1b;T}\tau}} = \gamma_0 e^{\tau(k_{1b;T}-k_{1a;T})} \qquad (22)$$

The parameter δ describing the ratio of β-citronellene (**2**) and isocitronellene (**3**) initially formed from **1** was introduced in eq 4. δ is a parameter picturing the reaction ratio of the two possible fragmentation routes (Scheme 1). Modeling the temperature dependency of δ, it is necessary to include consecutive reactions of **2** and **3** leading to side products **4** and **5**, respectively. The temperature dependent ratio of pathways I and II, δ_T, was calculated as presented in eq 23, wherein the molar fractions of **2** and **3** were calculated referring to eqs 24 and 25, respectively. Figure 6 compares δ_T from experiment and the kinetic model for five different substrates with γ_0 ranging from ∞ (pure **1a**) to 0 (pure **1b**). The visible discrepancies at T below

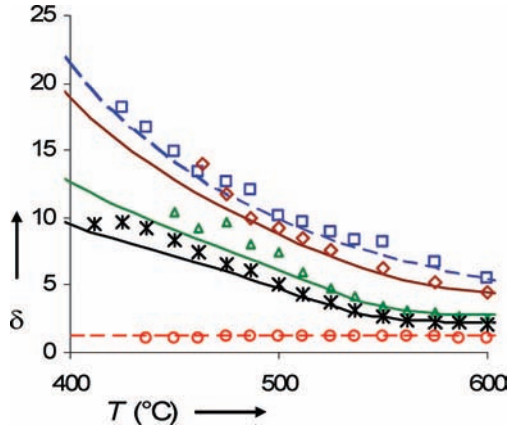

Figure 6. Ratio of β-citronellene (**3**) δ vs T for experimental data (symbols) and modeling data (lines) for different initial γ-values. *cis*-Pinane: $\gamma_0 \rightarrow \infty$, squares and dashed blue line; $\gamma_0 = 9.87$, diamonds and brown line; $\gamma_0 = 1.77$, triangles and green line; $\gamma_0 = 0.94$, asterisk and black line. *trans*-Pinane: $\gamma_0 \rightarrow 0$, circles and dashed red line.

SCHEME 4

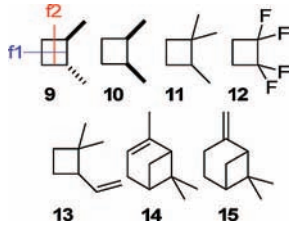

500 °C are due to limitations of the detection limit of the GC-FID. Because of the low concentration of the pyrolysis products (in particular **4** and **5**) the peaks were not detected until a limit for peak area and peak height is reached. Nevertheless, it is possible to model the temperature dependency of δ with the calculated activation parameters (Table 3), supporting the fact that the correct kinetic model for description of the pyrolysis process of both **1a** and **1b** was chosen.

$$\delta_T = \frac{[\mathbf{2}]_T}{[\mathbf{3}]_T} = \frac{[\mathbf{2}]_{\mathbf{1a};T} + [\mathbf{2}]_{\mathbf{1b};T}}{[\mathbf{3}]_{\mathbf{1a};T} + [\mathbf{3}]_{\mathbf{1b};T}} \quad (23)$$

$$[\mathbf{2}]_T = \frac{k_{\mathbf{2(1a)};T}[\mathbf{1a}]_0}{k_{\mathbf{1a};T}}(1 - e^{-k_{\mathbf{1a}}\tau}) + \frac{k_{\mathbf{2(1b)};T}[\mathbf{1b}]_0}{k_{\mathbf{1b};T}}(1 - e^{-k_{\mathbf{1b};T}\tau}) \quad (24)$$

$$[\mathbf{3}]_T = \frac{k_{\mathbf{3(1a)};T}[\mathbf{1a}]_0}{k_{\mathbf{1a};T}}(1 - e^{-k_{\mathbf{1a};T}\tau}) + \frac{k_{\mathbf{3(1b)};T}[\mathbf{1b}]_0}{k_{\mathbf{1b};T}}(1 - e^{-k_{\mathbf{1b};T}\tau}) \quad (25)$$

The temperature dependent parameter δ_T introduced with eq 23 describes the ratio between two possible decyclization routes for the unsymmetrical substituted cyclobutane ring in **1**. Fragmentation of four-membered rings in compounds with symmetrical substitution such as cyclobutane or **8** leads to identical products for both possible reaction channels.[18,19] In the case of 1,2-disubstituted cyclobutanes **9**−**13** pictured in Scheme 4 what kind of fragmentation products are formed via pyrolysis depends on which carbon bonds are cleaved. Reaction via route f1 leads to the formation of propene or 1,1-difluoroethene for **9**, **10**, or **12**, respectively,[26–28] and the decomposition of 1,1,2-trimethylcyclobutane (**11**) yields isobutene and propene.[29] Fragmentation via route f2 yields ethylene as one product and as the second product *trans*-butene, *cis*-butene, isoprene or perfluoroethylene for pyrolysis of **9**, **10**, **11**, or **12**, respectively.[26–29] Route f1 corresponds to the formation of **2** from **1** whereas reaction via f2 yields **3** when **1** is pyrolyzed.

TABLE 7: Ratio between Two Fragmentation Routes f1 and f2 (Scheme *4*) for Cyclobutane Derivatives 9−12[a] and the Ratio between 2 and 3 for 1a and 1b[b]

				f1/f2 or δ for T (°C)		
compound	ref	ΔM_{f1}[c]	ΔM_{f2}[c]	450	550	650
1b	this work			1.09	1.08	1.07
9	26	0	28 (C_2H_4)	3.40	2.92	2.60
10	27	0	28 (C_2H_4)	6.50	5.05	4.14
11	29	14 (CH_2)	42 (C_3H_6)	8.70	6.36	4.98
1a	this work			13.39	6.79	3.98
12	28	0	72	16.87	12.21	9.47

[a] Ratio of rate constants for the two fragmentation routes calculated for the given T. [b] k_2/k_3 for *cis*-pinene (**1a**) and *trans*-pinane (**1b**) based on the Arrhenius parameters listed in Table 3. [c] Mass difference between the products formed via fragmentation route f1 or f2 (Scheme 4) in units of relative molar mass.

SCHEME 5: Connection of Fragmentation Routes in the Case of Pinane (1) with Those Routes Reported for Fragmentation of Cyclobutane Derivatives (cf. Scheme 4, Table 7)[a]

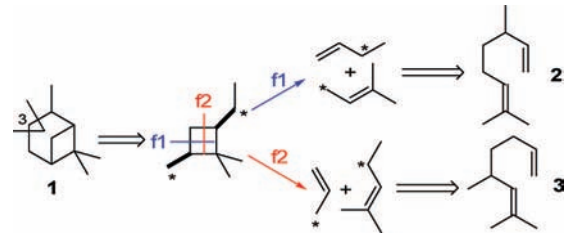

[a] Asterisks mark the place whereat the $C(3)H_2$ group in **1** was removed or reinserted.

Table 7 lists the ratio of the two possible fragmentation routes for compounds **9**−**12** expressed by the ratio of the rate constants calculated on the basis of published Arrhenius parameters in comparison with δ (eq 23) for rearrangement of **1a** and **1b**.[26–29] In general, the fragmentation routes leading to products with the same or similar molecular mass are preferred. The mass difference between products formed via f1 or f2 increases from **9** to **12**. Therefore, the ratio of both pathways is higher for **12** than for **9**, indicating that fragmentation route f1 is preferred. However, increasing T is connected with a decrease of the ratio f1/f2, which allows for the conclusion that pyrolysis at higher T yields both types of products in equal amounts.

Scheme 5 describes the relationship between **1** and the compounds sketched in Scheme 4. Removing C(3) leads to 2,2,3-trimethyl-1-ethylcyclobutane, which would yield two different sets of products if reaction proceeded via either route f1 or f2 (Scheme 5). Fragmentation route f1 leads to butene and 2-methylbut-2-ene, whereas propene and 2-methylpent-2-ene are formed if the reaction proceeds the other way (f2). Reconnection of the fragments by reintroduction of the CH_2 group at the marked atoms leads to **2** and **3**, respectively. With respect to these abstractions the preference of **2** for pyrolysis of **1a** is in accordance with the results concerning the pyrolysis of **9**−**12** (Table 7).[26–29] Pyrolysis of **1b** is exceptional because both fragmentation products are formed in nearly the same ratio (δ: 1). It has to be pointed out that pyrolysis of vinyl-substituted cyclobutane derivatives such as 1,1-dimethyl-2-vinylcyclobutane (**13**), α-pinene (**14**) or β-pinene (**15**) yield products formed via route f1 exclusively.[4,6,23,30] Whereas pyrolysis of **9**-**12** yields

fragmentation products almost exclusively,[26–29] the thermal treatment of **13**-**15** leads to products arising form sigmatropic-shift reactions also.[4,22,23]

Conclusion

For the first time a kinetic model for the thermal rearrangement of pinane (**1**) is presented, taking into account the different reactivities of the diastereoisomers *cis*- (**1a**) and *trans*-pinane (**1b**). Consecutive reactions of the primarily formed products β-citronellene (**2**) and isocitronellene (**3**) were also considered in the model. The experimental determination of the rate constants and activation parameters (Arrhenius and Eyring) were based on experiments carried out with the same apparatus and under identical reaction conditions. On the basis of a larger Arrhenius rate constant at a common temperature the higher reactivity of **1a** compared to the *trans*-isomer (**1b**) was confirmed.

The model of competitive first-order kinetics describes well the reaction of both **1a** and **1b**, supporting the hypothesis that the isomerization predominantly proceeds via stepwise fragmentation mechanisms of the cyclobutane ring. Hence, the Arrhenius and Eyring parameters indicate a tight transition state for the formation of the monocyclic *p*-menthene-type products their formation proceeds via a sigmatropic shift reaction rather than via the formation of a biradical. Activation parameters for reactions of **2** and **3** leading to consecutive products **4** and **5**, respectively, reveal that the reaction passes through a six-membered-ring transition state which is typical for ene-reactions. Comparison of experiments with different ratios of **1a** and **1b** shows that the results of kinetic model and experiment match over a wide temperature range.

Acknowledgment. We acknowledge the support given by Dr. M. M. Hoffmann (SUNY Brockport, New York) and thank Dr. T. Netscher (DSM, Switzerland) for the fruitful discussions and the helpful hints. Special thanks to the unknown referees whose comments helped to improve the manuscript.

Supporting Information Available: Plots used for calculation of the rate constants describing the disappearance of **1a**, **1b**, **2**, and **3** together with the calculated rate constants; the kinetic model for the thermally initiated gas-phase isomerization of *trans*-pinane (**1b**); and the optimized geometries of **1a**, **1b**, **2**, and **3**. This material is available free of charge via the Internet at http://pubs.acs.org.

References and Notes

(1) Banthorpe, D. A.; Whittaker, D. *Q. Rev.* **1966**, *20*, 373.
(2) Swift, K. A. D. *Top. Catal.* **2004**, *27*, 143.
(3) Thomas, A. F. *Pure Appl. Chem.* **1990**, *62*, 1369.
(4) Gajewski, J. J.; Kuchuk, I.; Hawkins, C. M.; Stine, R. *Tetrahedron* **2002**, *58*, 6943.
(5) Semikolenov, V. A.; Illína, I. I.; Simakova, I. L. *Appl. Catal., A* **2001**, *211*, 91.
(6) (a) Stolle, A.; Ondruschka, B.; Bonrath, W. *Eur. J. Org. Chem.* **2007**, 2310. (b) Stolle, A.; Ondruschka, B.; Findeisen, M., *Proceedings of the 3rd International Conference on Environmental Science and Technology, August 5−9, 2007, Houston, TX*; Starrett, S. K., Hong, J., Wilcock, R. J., Li, Q., Carson, J. H., Arnold, S., Eds.; American Science Press: Houston, 2007.
(7) Lemée, L.; Ratier, M.; Duboudin, J.-G.; Delmond, B. *Synth. Commun.* **1995**, *25*, 1313.
(8) Rienäcker, R. *Brennstoff-Chem.* **1964**, *45*, 20.
(9) Stolle, A.; Ondruschka, B.; Bonrath, W.; Netscher, T.; Findeisen, M.; Hoffmann, M. M. *Chem. Eur. J.*, submitted for publication.
(10) Rienäcker, R.; Ohloff, G. *Angew. Chem.* **1961**, *73*, 1369.
(11) Tanaka, J.; Katagiri, T.; Izawa, K. *Bull. Chem. Soc. Jpn.* **1970**, *44*, 130.
(12) Huntsman, W. D.; Lang, C. P.; Madison, N. L. Uhrick, D. A. *J. Org. Chem.* **1962**, *27*, 1983.
(13) Huntsman, W. D.; Curry, T. H. *J. Am. Chem. Soc.* **1958**, *80*, 2252.
(14) Stolle, A.; Brauns, C.; Nüchter, M.; Ondruschka, B.; Bonrath, W.; Findeisen, M. *Eur. J. Org. Chem.* **2006**, 3317.
(15) Roos, B. O. *Adv. Chem. Phys.* **1987**, *69*, 399.
(16) Weigand, E. F.; Schneider, H. *J. Org. Magn. Reson.* **1979**, *12*, 637.
(17) Gowenlock, B. G. *Q. Rev.* **1960**, *14*, 133.
(18) Walsh, R. *Chem. Soc. Rev.* **2008**, *37*, 686.
(19) Frey, H. M.; Walsh, R. *Chem. Rev.* **1969**, *69*, 103.
(20) Genaux, C. T.; Kern, F.; Walter, W. D. *J. Am. Chem. Soc.* **1953**, *75*, 6196.
(21) Kinzel, D. Unpublished results, Jena, 2008.
(22) Gajewski, J. J. *Hydrocarbon Thermal Isomerizations*, 2nd ed.; Elsevier Academic Press: San Diego, 2004; pp 46−50.
(23) Chickos, J. S.; Frey, H. M. *J. Chem. Soc., Perkin Trans. 2* **1987**, 365.
(24) Data taken from ref 13: $k = 6.65\times10^{-3}$ s^{-1} (382.5°C) and $k = 1.96\times10^{-2}$ s^{-1} (409.0°C). It has to be pointed out that the apparatus used in ref 13 is similar to that reported herein but the contact times were significantly longer (contact time: 31−60 s).
(25) Stolle, A. Unpublished results, Jena, 2007.
(26) Gerberich, H. R.; Walters, W. D. *J. Am. Chem. Soc.* **1961**, *83*, 4884.
(27) Gerberich, H. R.; Walters, W. D. *J. Am. Chem. Soc.* **1961**, *83*, 3935.
(28) Colin, R. T.; Frey, H. H. *J. Chem. Soc. Faraday I* **1980**, *76*, 322.
(29) Cocks, A. T.; Frey, H. M. *J. Phys. Chem.* **1971**, *75*, 1437.
(30) Hawkins, J. E.; Vogh, J. W. *J. Phys. Chem.* **1953**, *57*, 902.

JP800916B